Evaluation of a new approach for the injection performance simulation of autoinjectors

Felix Seiler

***Abstract*—There are already numerous approaches in the literature to explain and calculate injection times of autoinjectors. In addition to the forces used to extrude the syringe content, other parameters such as viscosity, needle properties, and others have also been considered. The new approach evaluated here relates to the characterization of the rear sub-assembly of an autoinjector, which contains the spring that exerts the force on the syringe. The results of the spring characterization are fed into a simulation method, which then simulates a real autoinjector by extruding the plain pre-filled syringe to calculate the injection time. These results are compared with the injection times of fully assembled autoinjectors and the simulation method is evaluated on this basis.**

I. Introduction

THE skin is the largest organ of the human body and it is the border between human and environment [1]. In addition to sensory and motor properties, the three layers form a mechanical and chemical protection against dangerous environmental influences. The top layer, the epidermis, is mainly responsible for the protective function. The middle layer, the dermis, serves primarily for immunological protection. The subcutis, which is the lowest layer, consists mainly of subcutaneous fatty tissue, serves as an energy reserve and provides insulation [2].

A. Motivation

Autoinjectors offer patients the opportunity to inject themselves with medications that need to be taken regularly. The application is relatively simple, the patient does not have to worry about the correct dosage or needle-stick injuries. Most autoinjectors are spring-driven [3], [4] and, because the needle is not visible, make it easy for the patient to overcome any fears associated with the injection [5]. According to [6], an auto-injector works as follows: Usually, the syringe inner wall is coated with silicone oil. Typically, the spring force is between 8 N and 50 N [7]. Inside the syringe, there is a space between the plunger and the fluid. When the auto-injector is activated, the spring deploys and moves the driving rod downward to eventually hit the plunger. The entire syringe moves towards the injection site and finally, the needle penetrates the skin. Then the plunger is pushed down by the spring until it reaches the tip of the barrel. Injection of the solution ends when the plunger reaches the lower end of the syringe [6].

Injection time is defined as the time it takes for the drug to be fully injected into the application site from activation. This is a very important parameter in the characterization of autoinjectors. Differences in performance between different autoinjectors can come, for example, due to variations in the composition of the drug contained, device components or environmental influences. For this reason, it is important to identify the factors that influence injection time and to include them in the development. The extent of the influence of the various factors is also important [8]. One challenge in development is that particularly high-viscosity drugs require a relatively high spring force to keep the injection time within a comfortable range for the patient [6]. The large spring force required can cause problems in that the mechanical load on the plastic housing can also cause problems concerning the bearing [9]. Fischer et al. [7] and Thueer et al. [8] have already developed models to predict injection forces and injection time. The force required for injection depends on the targeted injection time, injection volume, drug viscosity, and injection rate, which also affects handling [10], [11], [12]. The pain perceived by the patient during the injection is mainly related to the injection rate. Pain-free injections are possible with injections of a maximum of 1 mL injection volume and an injection rate of 0.1 mL/min [13]. Patients do not want an injection time which is longer than 15 seconds [14]. Long injection times can also be dangerous, as evidenced by the fact that 76% of application errors occur because the patient is unable to hold the device at the injection site to inject the required amount of drug [15]. Analysis of autoinjector behavior has been part of several studies. Some models are based, for example, on the equilibrium of static forces, which also take into account the friction of the stopper as well as the pressure drop along the needle. The basis here is the Hagen-Poiseuille equation [16]. Various authors have studied the influence of different parameters on the performance of autoinjectors. Among them, the variability of components has been studied, as they can provide information on the injection time. The behavior of non-Newtonian fluids has also been studied [16], [17], [18], [19], [20], [21]. Internal friction has a greater influence in injection devices with a threaded system, such as insulin pens. This factor plays a rather minor role in autoinjectors [22]. The properties of proteins have a significant influence on the behavior of protein solutions in syringes. Highly concentrated formulations in particular have special rheological properties. These challenges come from critical stability of the formulation, manufacturability, and patient application. Rathore et al. [21] have studied protein-device combinations with respect to three factors: The authors found that interactions between product and syringe surface can affect the frictional force. Their results show that highly viscous drugs exhibit strong shear-thinning behavior, which

F. Seiler is student of the Master's program Medical Technologies, MCI, Innsbruck, Austria, e-mail: f.seiler@mci4me.at.

has a major impact on injection time as well as hydrodynamic forces. These shear-thinning properties lead to the forces required for extrusion being estimated to be larger than they actually are [20], [21]. The total force for injections consists of three components: The force coming from the tissue resistance [10], the force due to friction between the plunger and the barrel [6], and the hydrodynamic force [15]. Fischer et al. [7] empirically determined that it is important to know the exact dimensions of the needle in order to determine the injection forces. Also Verwulgen et al. [15] confirm that the needle has a large influence on the injection parameters, because the thinner the needle is, the larger the force must be for the injection. The composition of the drug as well as the dynamic viscosity play a role in the size of the needle inner diameter, thus drugs with larger molecules and higher viscosity require a larger diameter [12]. All components of such an injection system have inherent variability that needs to be assessed and their influence on the overall injection determined [17]. In the course of their study, Rathore et al. [17] found that variation of the needle alone can cause a 30% increase in injection time. Variability in other components as well as variations in measurements can also cause significant errors. For viscous fluids, the predominant factors in injection time are spring tension, product concentration, and needle size. In the worst case, 80% variability in force can result in 80% variability in injection time. To model friction, a friction coefficient can be used in combination with a normal force, which is an approach to calculate dry friction [22]. However, the inner wall of a syringe in an autoinjector is siliconized. For this reason, the model for plug friction must apply to wet friction, which depends on velocity [19]. Furthermore, compression of the stopper, which occurs when the syringe is extruded, results in radial deformation. This increases the normal force at the surface where the syringe wall is in contact with the stopper. This can lead to higher friction [8]. Since the autoinjector is driven by a spring, this spring force is the input variable for the model used to calculate the injection time [18], [19].

B. Goal of the study

The autoinjector must always be matched to the drug with which it is used, as stronger springs must be used for more viscous drugs, for example. Up to now, the decision for the spring force or the corresponding component of the autoinjector has been based primarily on experience and estimates. If this decision is wrong, the entire assembled batch (autoinjector + syringe) cannot be released for sale, as it then does not meet the requirements. To avoid this, the aim of this study is to test the individual components of the combination product before assembly to avoid errors in production.

II. Materials and methods

A. Syringes

For all experiments, pre-fillable syringes from the manufacturer Becton Dickinson (BD) of the type BD Hypak® with a filling volume of 1 mL were used with a staked-on 27G needle with an inner needle diameter of 0.24 mm and a needle length of 19 mm. The inner diameter of the syringe barrel is 6.35 mm. The stoppers are of type BD FluroTec® 4023/50.

B. Surrogate solutions

A hydroxypropyl methylcellulose (HPMC) solution is prepared as it also exhibits non-Newtonian, shear thinning behavior. The target viscosity is 8.5 mPa·s (±0.5 mPa·s) at a target concentration of 1.3% HPMC. Viscosity measurements at the end of the compounding process gave values of 8.39 mPa·s at 23.0° C and 9.35 mPa·s at 18.0° C for the first batch of HPMC, the second batch showed viscosities of 8.59 mPa·s at 23.0° C and 9.38 mPa·s at 18.0° C, respectively.

C. Autoinjectors

Basically, the autoinjectors used here consist of three components: The front sub-assembly (FSA), the rear sub-assembly (RSA) and the pre-filled syringe (PFS). These three components are assembled into the finished product. The RSA contains a spring that drives the plunger rod contained in the FSA after activation. The three components can be combined in different designs depending on the requirements.

D. Test methods

Both assembled autoinjectors and pre-filled syringes (PFS) are tested with linear materials testing machines from the manufacturer Zwick Roell. The samples are stored at two different conditions: 18.0° C or 23.0° C and 50.0% relative humidity. They are always taken out right before testing.

1) Functional autoinjector test (FT): This test setup is used to measure the injection time of assembled autoinjectors. Basically, an autoinjector is held and moved linearly vertically downwards until its needle cover arrives at the resistance plate. Various sensors (cameras, lasers, scales) detect the injection that then takes place and measure various parameters, which will be discussed in more detail below. The autoinjector is clamped in the machine in such a way that there is a defined distance between the needle cover and the resistance plate. This distance is ensured by means of a spacer, which is placed between the resistance plate and the autoinjector. The autoinjector is then clamped by means of the pneumatic holders. A collecting container underneath the autoinjector catches the expelled fluid, the weight of which is recorded by the scale. The start and end time of the extracted liquid is determined by means of a light barrier. The autoinjector is attached to a crosshead which moves vertically downwards and encloses a force sensor. The autoinjector is activated when the needle cover hits a plate. After successful injection, the crosshead moves up again a little way and then moves back towards the resistance plate to measure the displacement of the now locked needle cover shield. The crosshead then moves back to the start position and the measurement of a sample is completed.

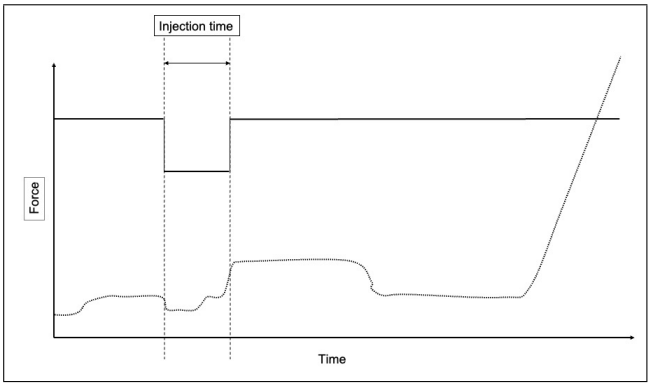

Fig. 1. Schematic functional testing diagram for an autoinjector. Solid line: light barrier. Dotted line: force.

2) Plunger rod force profile test (SAR): This method is used to determine the force profile of the RSA, the force of the plunger is measured directly after the activation of the device. For this test, the autoinjectors are not assembled with filled PFS, but with so-called dummies, which have no needle. The force profile, which can be seen in figure 2, is then used to simulate an autoinjector. Initially, the crosshead travels vertically in the direction of the clamped autoinjector. The activation actuator pushes down the needle cover of the autoinjector, activating the autoinjector. At this point, the actual measurement starts. This causes the plunger to come up, and the compression die follows it and measures the force profile.

Fig. 2. Schematic SAR diagram for an autoinjector. Plunger rod force and indicators.

3) Break-loose gliding force test (BLGF): In this test method, PFS are extruded at a defined speed of 190 mm/s, and the break-loose force and the extrusion/gliding force are measured. The behavior during the test can be seen in Figure 3.

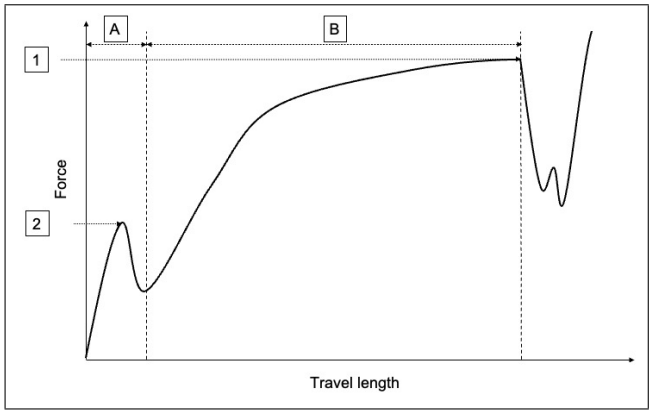

Fig. 3. Schematic force diagram for a pre-filled syringe.

4) Spring simulation test (SST): In contrast to the BLGF method, in the SST method the PFS are not measured with a defined velocity, but with a defined force profile, in this case of 12 - 8.5 N. The force profile of the RSA determined by the SAR method is also fed into the method. This method can be used to simulate various parameters of an autoinjector, including injection time, glide force, friction force of the stopper, and inner needle diameter. For this purpose, a syringe profile $S_M(x)$ is calculated, which is the ratio of the real measured force $F_M(x)$ during extrusion by the velocity.

$$S_M(x) = \frac{F_M(x)}{V(x)} \tag{1}$$

This syringe profile serves as the fingerprint of the PFS. From this syringe profile, in combination with the force profile of the RSA, the injection time can be calculated. The friction force of the stopper as well as the inner needle diameter are obtained by subtracting the total force from the hydrodynamic force determined by the Hagen-Poiseuille equation. In figure 4 the test procedure can be obtained which is divided in different phases: A) Approach, B) Compression, C) Pseudo-linear, D) Syringe extrusion, E) Air extrusion.

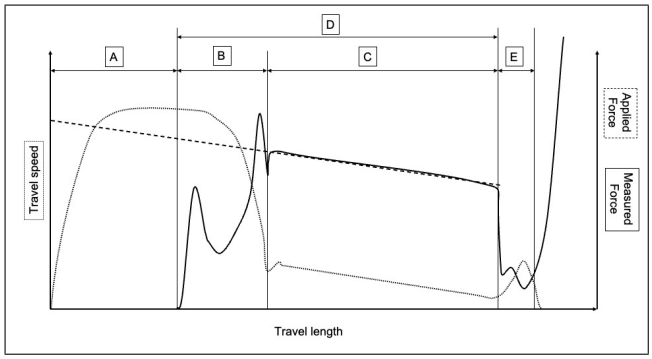

Fig. 4. Schematic SST diagram for a pre-filled syringe.

E. Component combination and indexing

The different components are combined and indexed in the following way for further reference:

TABLE I
COMPONENT COMBINATIONS AND TEST INDEXING.

Index	PFS	FSA	RSA	Temp. / °C
Configuration 1	PFS 1	FSA 1	RSA 1	18
Configuration 2	PFS 1	FSA 1	RSA 1	23
Configuration 3	PFS 2	FSA 1	RSA 1	18
Configuration 4	PFS 2	FSA 1	RSA 1	23
Configuration 5	PFS 3	FSA 1	RSA 1	18
Configuration 6	PFS 3	FSA 2	RSA 1	23
Configuration 7	PFS 4	FSA 2	RSA 1	18
Configuration 8	PFS 4	FSA 1	RSA 2	23
Configuration 9	PFS 5	FSA 2	RSA 1	18
Configuration 10	PFS 5	FSA 1	RSA 1	23
Configuration 11	PFS 6	FSA 3	RSA 3	18
Configuration 12	PFS 6	FSA 3	RSA 3	23
Configuration 13	PFS 7	N/A	N/A	18
Configuration 14	PFS 7	N/A	N/A	23

III. RESULTS

A. Theoretical simulation of injection parameters

1) Simulation of force vs. flow rate: This equation is used to calculate the extrusion force as a function of speed. The basis is the Hagen-Poiseuille equation, which relates the flow of a fluid through a needle to the radius of the needle, the pressure difference between the two ends, the needle length, and the viscosity of the fluid. The final equation relates the force applied by the plunger to the propulsion speed of the stopper and shows a linear relationship between these parameters. This simulation takes into account only hydrodynamic forces and not frictional forces.

$$F = \frac{\Delta d}{\Delta t} \cdot \frac{\eta \cdot l \cdot D^4 \cdot \pi}{2 \cdot r^4} \tag{2}$$

2) Simulation of the stopper displacement vs. time in a spring-driven syringe: To calculate the displacement over time in a spring-driven syringe, the equation 2 is solved for Δd. By knowing the initial spring force at displacement 0 and the force of the spring at a partial extension of the spring, the equation can be solved using an iterative approach:

$$\Delta d_1 = \frac{0.1\,s \cdot 2 \cdot r^4 \cdot (F_0 - k \cdot d_0)}{\eta \cdot l \cdot D^4 \cdot \pi} \tag{3}$$

$$d_{0.1\,s} = d_0 + \Delta d_1 \tag{4}$$

Starting from this new location $d_{0.1\,s}$, which the stopper has reached after 0.1 s, the force was calculated, which the now slightly more extended spring shows ($F_0 - k \cdot d_{0.1\,s}$). From this new spring force, the position of the stopper after 0.2 s ($d_{0.2\,s}$) was calculated:

$$\Delta d_2 = \frac{0.1\,s \cdot 2 \cdot r^4 \cdot (F_0 - k \cdot d_{0.1\,s})}{\eta \cdot l \cdot D^4 \cdot \pi} \tag{5}$$

$$d_{0.2\,s} = d_{0.1\,s} + \Delta d_2 \tag{6}$$

3) Calculation of the injection time of a spring-driven syringe: If the previous numerical solution is transformed into a differential equation, the displacement d_t for a given time t can be described as follows:

$$d_t = d_0 \cdot e^{-\frac{2 \cdot r^4 \cdot k}{\eta \cdot l \cdot D^4 \cdot \pi} \cdot t} - \frac{F_0}{k} \cdot (e^{-\frac{2 \cdot r^4 \cdot k}{\eta \cdot l \cdot D^4 \cdot \pi} \cdot t} - 1) \tag{7}$$

Solving this equation after t leads to

$$t = ln\left(\frac{d_0 \cdot k - F_0}{d_t \cdot k - F_0}\right) \cdot \frac{\eta \cdot l \cdot D^4 \cdot \pi}{r^4 \cdot 2 \cdot k} \tag{8}$$

for a certain stopper start position d_0 and a certain stopper end position d_t.

B. Injection time

To assess the validity of the SST method in terms of its ability to predict autoinjector injection time, the measured FT method injection times were statistically evaluated against the SST method results. Comparisons were made per PFS batch and per temperature (18.0 and 23.0° C, respectively). Means and standard deviations were determined and compared by t-test at a significance level of 0.05 using MatLab software (version 2021a, MathWorks Inc.).

The hypotheses for the statistical evaluation are defined as follows:

- H_0 : There is no difference in the method with regard to the injection time. The mean in the FT method equals the mean in the SST method.
- H_1 : There is a difference in the method with regards to the injection time. The mean in the FT method does not equal the mean in the SST method.

The results can be obtained in table II where significant differences are marked with an asterisk *.

TABLE II
RESULTS IT METHOD COMPARISON. DEVIATIONS BETWEEN SST AND FT METHOD.

Config.	Temp. in °C	Visc. in mPa·s	IT in %
1	18	9.68	-0.40
2	23	8.13	-5.54*
3	18	10.00	-4.76*
4	23	8.40	3.90*
5	18	9.99	-2.40
6	23	8.40	2.16
7	18	9.65	-1.00
8	23	8.07	1.84
9	18	9.71	-0.42
10	23	8.13	1.84
11	18	9.35	1.65
12	23	8.39	2.13

C. Gliding force

To assess the validity of the SST method in terms of its ability to predict autoinjector gliding force, the measured BLGF method injection times were statistically evaluated against the SST method results. Comparisons were made per PFS batch and per temperature (18.0 and 23.0° C, respectively). Means and standard deviations were determined and compared by t-test at a significance level of 0.05 using MatLab software (version 2021a, MathWorks Inc.).

The hypotheses for the statistical evaluation are defined as follows:

- H_0 : There is no difference in the method with regard to the gliding force. The mean in the BLGF method equals the mean in the SST method.

- H_1 : There is a difference in the method with regards to the gliding force. The mean in the BLGF method does not equal the mean in the SST method.

The results can be obtained in table III where significant differences are marked with an asterisk *.

TABLE III
RESULTS GF METHOD COMPARISON. DEVIATIONS BETWEEN SST AND BLGF METHOD.

Config.	Temp. in °C	Visc. in mPa·s	GF in %
1	18	9.68	-3.18
2	23	8.13	-13.55*
3	18	10.00	-6.43*
4	23	8.40	-1.67
5	18	9.99	-3.54*
6	23	8.40	-4.98*
7	18	9.65	-3.48*
8	23	8.07	-0.05
9	18	9.71	-0.26
10	23	8.13	-0.12
11	18	9.35	7.18*
12	23	8.39	7.71*

D. Stopper friction

The SST method is used to calculate the frictional force of the stopper on the syringe wall. The results are determined for each of the two temperatures and any statistical differences are determined using analysis of variance (ANOVA) at a significance level of 0.05.

The hypotheses for the statistical evaluation are defined as follows:

- H_0 : There is no difference in the means of $F_{Stopper}$ between the different configurations.
- H_1 : There is a difference in the means of $F_{Stopper}$ between the different configurations.

The results can be obtained in table IV and show a statistically significant difference (P<0.001) in the stopper friction between the measurements.

TABLE IV
RESULTS STOPPER FRICTION FORCE.

Config.	Temp. in °C	Visc. in mPa·s	$F_{Stopper}$ in N
1	18	9.68	3.61
2	23	8.13	3.65
3	18	10.00	4.04
4	23	8.40	4.50
5	18	9.99	4.32
6	23	8.40	4.85
7	18	9.65	4.58
8	23	8.07	4.31
9	18	9.71	4.13
10	23	8.13	4.93
11	18	9.35	4.53
12	23	8.39	4.63
13	18	9.38	4.69
14	23	8.59	4.20

E. Inner needle diameter

The inner needle diameter is determined using the SST method. The results are statistically analyzed by ANOVA at a significance level of 0.05.

The hypotheses for the statistical evaluation are defined as follows:

- H_0 : There is no difference in the means of d_{Needle} between the different configurations.
- H_1 : There is a difference in the means of d_{Needle} between the different configurations.

The results can be obtained in table V and show a statistically significant difference (P<0.001) in the mean of the inner needle diameter between the measurements.

TABLE V
RESULTS INNER NEEDLE DIAMETER.

Config.	Temp. in °C	Visc. in mPa·s	d_{Needle} in mm
1	18	9.68	0.229
2	23	8.13	0.234
3	18	10.00	0.225
4	23	8.40	0.223
5	18	9.99	0.227
6	23	8.40	0.230
7	18	9.65	0.232
8	23	8.07	0.226
9	18	9.71	0.237
10	23	8.13	0.244
11	18	9.35	0.241
12	23	8.39	0.239
13	18	9.38	0.240
14	23	8.59	0.246

IV. DISCUSSION

Using the Hagen-Poiseuille equation as a starting point, injection time calculations can be performed if certain geometric parameters of the syringe and thermal and rheometric properties of the fluid are known. Although the results of the theoretical considerations represent a good starting point for further experimental investigations, only frictionless cases can be simulated with these calculations, furthermore no highly viscous fluid but only water was included in the consideration.

It is known that a frictional force is present during the extrusion of a syringe. The tests performed in this study show values for the friction of the stopper against the inner wall of the syringe barrel of about 3.6 to 5 N. The force applied in the SST method is up to 12 N, with the frictional force accounting for almost a quarter. Since both the frictional forces and the hydrodynamic factors are not constant over all tested objects and autoinjectors in particular are subject to many influencing factors, a theoretical prediction can only be made to a limited extent.

The force exerted on the PFS by the spring contained in the RSA of the autoinjector, which serves as an input parameter for the SST method, is crucial for the accurate determination of injection time, glide force, friction force and inner needle diameter. The injection time results obtained by both methods agree well. In figure 5 it can be observed that the injection time is influenced by the viscosity of the liquid as a higher viscosity is causing a longer injection time, the correlation coefficient between those two parameters is 0.45.

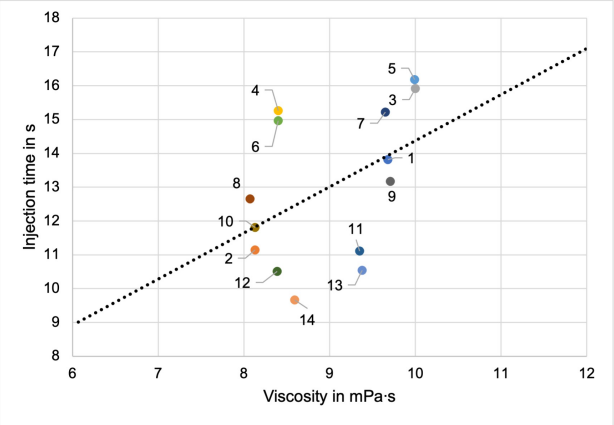

Fig. 5. Injection time over viscosity.

The aim was to predict the injection time using the SST method, which can be measured using the FT method. Seven of twelve comparisons showed no significant differences at a significance level of $\alpha = 0.5$. Two of the three comparisons where significant differences were present occurred in the same batch. This suggests that the differences occurred less because of the simulation method and more because of other factors. Also given the fact that the deviations of the injection time from one method to another is not more or less severe for the mAb solution to the surrogate solution. Determining these factors may serve as a guide for subsequent research, as the factors are numerous but not yet sufficiently proven as they differ between different research works [20], [21], [8]. Zhong et al. [6] have also developed an *in situ* dynamic model for spring-driven autoinjectors. However, this model has weaknesses compared to the methods described here in that a very large number of input parameters are required to make a reliable statement, for example, about the injection time. In contrast, parameters that are relatively easy to determine experimentally are sufficient for the process dealt with in this study, which also has a direct advantage for industrial applications and not only for scientific operations. Allmendinger et al. [20] have investigated and compared the injection properties of Newtonian and non-Newtonian fluids. Unlike other researchers, they also included surrogate solutions, which was also practiced in this study, albeit with different substances. A key point of this study is that viscosity shear rate profiles were also included in the calculations, which has a significant impact on both the extrusion speed and the resulting parameters.

In case of this study, basically the same product, the same syringes, the same stoppers, the same needles, the same storage conditions, the same machines, and the same test methods were used for all experiments. Of course, variations can also occur during the production of drug product and syringes with accessories over time and between different batches, the syringes may differ in terms of the siliconization of their inner wall, which may affect the frictional force of the stopper, the needles may differ minimally in their inner diameter, which may favor a possible clogging of the fluid in the needle, and also theoretically deviations may occur during the production of the drug product, which however, due to the very strict quality control in the pharmaceutical field, may only occur very minimally and in very exceptional cases.

In addition to the injection time, the glide force was also investigated in this study. In figure 6, it can be observed that the viscosity of the liquid contained in the syringe contributes to the gliding force as a higher viscosity is causing a higher gliding force, the correlation coefficient between those two parameters is 0.52.

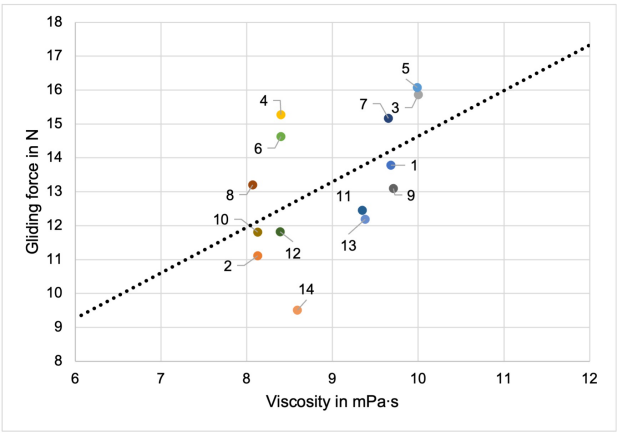

Fig. 6. Gliding force over viscosity.

The gliding force is a widely used parameter for characterizing pre-filled syringes. Classically, the glide force is performed as part of a break-loose and gliding force test. Since the test procedure is very similar for the BLGF and SST methods, the glide force can also be determined within the SST method. The two methods differ in the sequence control. While the control in the BLGF method is speed-dependent, the control in the SST method is force-dependent. The results for the determined glide force with both methods were evaluated and compared with each other. Significant differences in the results of the glide force were found for 7 of 12 tested configurations with 40 samples each at a significance level of $\alpha = 0.05$. The largest deviation was found in the configuration with the largest deviation in the injection times. However, this configuration does not exhibit a noticeably high viscosity, a high stopper friction or a small inner needle diameter. This observation leads to the assumption that there are other properties which significantly influence the injection parameters. In figure 7 it can also be seen that the injection time and the gliding force are closely linked together, higher gliding force implies a longer injection time, the correlation coefficient between those two parameters is 0.96.

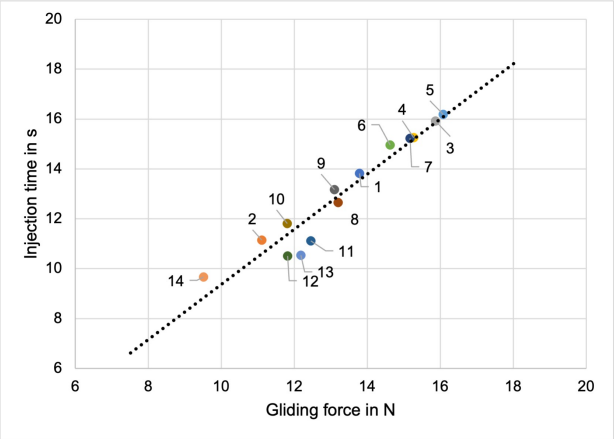

Fig. 7. Injection time over gliding force.

In addition to the injection time and the glide force, the SST method can also be used to determine the friction force of the stopper on the inner wall of the syringe barrel and the effective inner diameter of the needle. The determination of the friction force of the stopper on the inner wall of the syringe barrel and the effective inner diameter of the needle using the SST method is advantageous in that previous approaches, for example for the determination of friction forces, have always assumed additional equipment [6], [17], [21]. In contrast, the friction force in this method is calculated by subtracting the hydrodynamic forces from the total force. By using this method, the proportion of the stopper's frictional force to the total force can be clearly delineated from the hydrodynamic component. The determination of this parameter is important to distinguish whether a potentially problematic, because possibly too high, injection time or gliding force measurement can rather be attributed to the material or the injection solution. Thueer et al. [8] have also experimentally determined the friction of the stopper. However, they did not use a syringe filled with liquid but with air, which simulates the hydrodynamic pressure by means of a compressed air generator at the end of the needle. This approach has the advantage that the pressure can be made variable; on the other hand, more complex, non-Newtonian fluids in particular have to be simulated because of their shear-thinning behavior, among other things. A real correlation between stopper friction force and injection time or gliding force could not be proven with correlation factors close to zero. The ANOVA which was performed over the $F_{Stopper}$ measurements showed a significant difference between the means which does not prove the invalidity of the method but shows that different syringe batches present different levels of siliconization.

This effective needle inner diameter represents a valid reference point for estimating the injection performance. In figure 8, the correlation between the inner needle diameter and the injection time is displayed, the correlation coefficient between those two parameters is -0.82. This proves the assumption that a larger inner needle diameter decreases the injection time tremendously, as according to the Hagen-Poiseuille law the pipe radius even contributes with the fourth power. The ANOVA performed to compare the results showed a significant difference between the d_{Needle} means which can be due to different obstruction levels inside the needle. Also, the obtained inner needle diameter is highest in the surrogate solution syringes which might be due to clogging that occurs in the syringes with the protein solution.

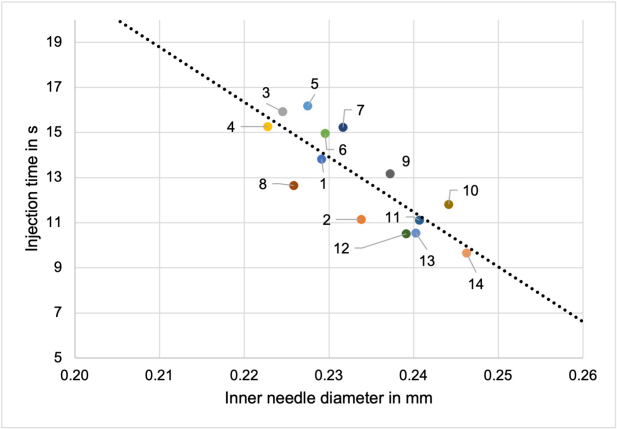

Fig. 8. Injection time over inner needle diameter.

As the inner needle diameter directly contributes to the hydrodynamic force which occurs during the extrusion of a syringe, the correlation between the gliding force and the inner needle diameter is displayed in figure 9. It can be observed that a smaller inner needle diameter causes a higher gliding force, the correlation coefficient between those two parameters is -0.83.

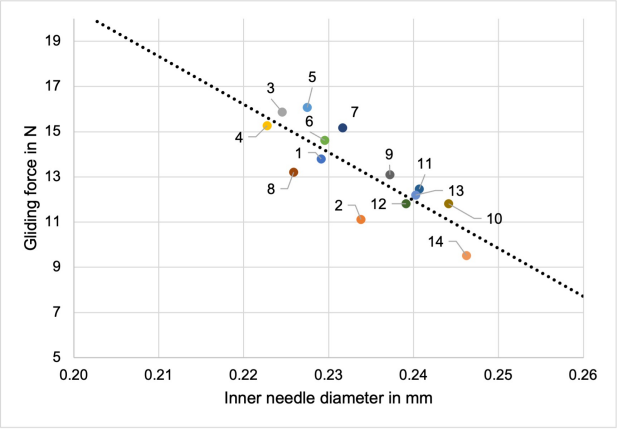

Fig. 9. Gliding force over inner needle diameter.

V. Conclusion and Outlook

In this study, different methods for characterization and evaluation of pre-filled syringes with mAb solution and surrogate solution in autoinjectors were investigated. It was found that reliable predictions about the performance of assembled combination products can be made using the spring simulation method. For this purpose, it is only necessary to characterize the spring contained in the rear sub-assembly of the autoinjector in advance, after which the bare PFS can be measured using a relatively simple test setup.

Above all, the results of the injection time, which is ultimately the decisive characteristic of an autoinjector, are very reliable. The glide force, which is the industry standard parameter for assessing PFS, can also be determined using the SST method as well as the proven BLGF method, for which the same test setup is used. In addition to these two main parameters, reasonable values could also be determined for the friction of the stopper on the inner wall of the syringe barrel as well as for the needle inner diameter. The tests described here were not only carried out with mAb solutions, but surrogate solutions were also used, which should improve the evaluation of the material (syringes and autoinjectors) in the future due to better controllable and more constant fluid dynamic properties.

The purpose of developing the SST method was originally to be able to make predictions about the injection time of an autoinjector with PFS before the autoinjector is finally assembled. Now, in this case, if the results of the simulation method show that the injection time is likely to be too large with the RSA used, a stronger RSA can be used for production to bring the injection times to an acceptable level. This results in large cost savings in real-world operations, as the appropriate components can be selected prior to production. An even better prediction can be made if even more influencing factors and on the injection time and also the extent of these factors are known and can be included in the simulation. All in all, however, the results of this study clearly show that the SST method is a very valid means of already fulfilling this purpose to a sufficient extent.

As described in the literature review, there are already models that also take into account the resistance of the tissue being injected [10], [13], [23]. The inclusion of tissue resistance is interesting in the sense that there are numerous in-house observations, e.g., in the context of human factors studies, that indicate a significant (in some cases doubled) increase in injection time compared to that measured in air. The SST method described in this paper could also be extended to include an investigation of tissue resistance and its associated effects. For this purpose, a suitable holder can be mounted below the syringe holder, which can accommodate a predefined piece of tissue. Theoretically, both artificial and natural tissues can be used. The advantage of artificial (e.g. gelatin-based) tissues is a better reproducibility of results. However, due to the fact that human respectively animal skin is a very complex construct, it can be difficult to sufficiently take into account the influencing factors of the different skin layers. Since the injections considered here are subcutaneous injections, the epidermis as well as the dermis must also be taken into account when creating an artificial skin or tissue model. Another point that must be considered is the possible difference between living and dead tissue. The research that has looked at subcutaneous injections in minipigs can be used as a guide to further investigate the differences between living and dead tissue. Furthermore, it would be beneficial if different tissue types (for example, with different levels of fat and muscle) were studied.

Another aspect that should be considered in future research on this topic is the effect of aging on the injection performance of PFS with mAb solutions in autoinjectors. Besides the possible change of the protein solution itself (physical parameters such as viscosity, but also pharmacological parameters and efficacy), the possible time-dependent change of the mechanical components (plastic components, spring, porosity of the stopper, tightness of the rigid needle shield) and especially the siliconization of the inner wall of the syringe barrel should be investigated.

REFERENCES

[1] A. Slominski, J. Wortsman, R. Paus, P. M. Elias, D. J. Tobin, and K. R. Feingold, "Skin as an endocrine organ: implications for its function," *Drug Discovery Today: Disease Mechanisms*, vol. 5, no. 2, pp. 137–144, 2008.

[2] J. E. Lai-Cheong and J. A. McGrath, "Structure and function of skin, hair and nails," *Medicine (United Kingdom)*, vol. 45, no. 6, pp. 347–351, 2017.

[3] I. Thompson and J. Lange, "Pen and Autoinjector Drug Delivery Devices," in *Sterile Product Development*, 6th ed., P. Kolhe, M. Shah, and N. Rathore, Eds. New York: Springer, 2013.

[4] A. Ravi, D. Sadhna, D. Nagpaal, and L. Chawla, "Needle free injection technology: A complete insight," *International Journal of Pharmaceutical Investigation*, vol. 5, no. 4, p. 192, 2015.

[5] C. Berteau, F. Schwarzenbach, Y. Donazzolo, M. Latreille, J. Berube, H. Abry, J. Cotten, C. Feger, and P. E. Laurent, "Evaluation of performance, safety, subject acceptance, and compliance of a disposable autoinjector for subcutaneous injections in healthy volunteers," *Patient Preference and Adherence*, p. 379, 2010.

[6] X. Zhong, T. Guo, P. Vlachos, J. C. Veilleux, G. H. Shi, D. S. Collins, and A. M. Ardekani, "An experimentally validated dynamic model for spring-driven autoinjectors," *International Journal of Pharmaceutics*, vol. 594, p. 120008, 2021.

[7] I. Fischer, A. Schmidt, A. Bryant, and A. Besheer, "Calculation of injection forces for highly concentrated protein solutions," *International Journal of Pharmaceutics*, vol. 493, no. 1-2, pp. 70–74, 7 2015.

[8] T. Thueer, L. Birkhaeuer, and D. Reilly, "Development of an advanced injection time model for an autoinjector," *Medical Devices: Evidence and Research*, vol. 11, pp. 215–224, 2018.

[9] A. Siew, "Building a better self-injection solution," *Pharmaceutical Technology*, vol. 40, pp. 18–23, 2016.

[10] A. Allmendinger, R. Mueller, E. Schwarb, M. Chipperfield, J. Huwyler, H. C. Mahler, and S. Fischer, "Measuring tissue back-pressure - In vivo injection forces during subcutaneous injection," *Pharmaceutical Research*, vol. 32, no. 7, pp. 2229–2240, 7 2015.

[11] V. Burckbuchler, G. Mekhloufi, A. P. Giteau, J. L. Grossiord, S. Huille, and F. Agnely, "Rheological and syringeability properties of highly concentrated human polyclonal immunoglobulin solutions," *European Journal of Pharmaceutics and Biopharmaceutics*, vol. 76, no. 3, pp. 351–356, 2010.

[12] M. Adler, "Challenges in the development of pre-filled syringes for biologics from a formulation Scientist's point of view," *American Pharmaceutical Review*, vol. 15, no. 1, p. 96, 2012.

[13] J. Gupta, S. S. Park, B. Bondy, E. I. Felner, and M. R. Prausnitz, "Infusion pressure and pain during microneedle injection into skin of human subjects," *Biomaterials*, vol. 32, no. 28, pp. 6823–6831, 2011.

[14] A. Fry, "Injecting highly viscous drugs," *Pharmaceutical Technology*, vol. 38, no. 22, 2014.

[15] S. Verwulgen, K. Beyers, T. Van Mulder, T. Peeters, S. Truijen, F. Dams, and V. Vankerckhoven, "Assessment of Forces in Intradermal Injection Devices: Hydrodynamic Versus Human Factors," *Pharmaceutical Research*, vol. 35, no. 6, 6 2018.

[16] N. Ajaghari and J. Authelin, "Modeling of autoinjectors," in *PDA Parenteral Packaging*, Venice, 2016.

[17] N. Rathore, P. Pranay, B. Eu, W. Ji, and E. Walls, "Variability in syringe components and its impact on functionality of delivery systems," *PDA Journal of Pharmaceutical Science and Technology*, vol. 65, no. 5, pp. 468–480, 2011.

[18] J. Wilkins and I. Simpson, "Mathematical Modelling for Faster Auto-Injector Design," *Drug Development & Delivery*, vol. 12, no. 6, pp. 41–45, 2012.

[19] A. Kivitz and O. G. Segurado, "HUMIRA Pen: a novel autoinjection device for subcutaneous injection of the fully human monoclonal antibody adalimumab," *Expert Rev Med Devices*, vol. 4, no. 2, pp. 109–116, 2007.

[20] A. Allmendinger, S. Fischer, J. Huwyler, H. C. Mahler, E. Schwarb, I. E. Zarraga, and R. Mueller, "Rheological characterization and injection forces of concentrated protein formulations: An alternative predictive model for non-Newtonian solutions," *European Journal of Pharmaceutics and Biopharmaceutics*, vol. 87, no. 2, pp. 318–328, 2014.

[21] N. Rathore, P. Pranay, J. Bernacki, B. Eu, W. Ji, and E. Walls, "Characterization of protein rheology and delivery forces for combination products," *Journal of Pharmaceutical Sciences*, vol. 101, no. 12, pp. 4472–4480, 2012.

[22] J. Lange, L. Urbanek, and S. Burren, "Development of devices for self-injection: Using tribological analysis to optimize injection force," *Medical Devices: Evidence and Research*, vol. 9, pp. 93–103, 2016.

[23] A. Allmendinger and S. Fischer, "Tissue Resistance during Large-Volume Injections in Subcutaneous Tissue of Minipigs," *Pharmaceutical Research*, vol. 37, no. 10, 10 2020.